

## CREATING AN EUV MASK MICROSCOPE FOR LITHOGRAPHY GENERATIONS REACHING 8 NM

Kenneth A. Goldberg<sup>1</sup>, Iacopo Mochi<sup>1</sup>, Markus P. Benk<sup>1</sup>, Arnaud P. Allezy<sup>1</sup>,  
Nathan S. Smith<sup>1</sup>, Carl W. Cork<sup>1</sup>, William Cork<sup>1</sup>, James Macdougall<sup>1</sup>,  
Weilun L. Chao<sup>1</sup>, Erik H. Anderson<sup>1</sup>, Patrick P. Naulleau<sup>1</sup>, Eric Acome<sup>2</sup>,  
Eric Van Every<sup>2</sup>, Alex Deyhim<sup>2</sup>, Veljko Milanovic<sup>3</sup> and Senajith B. Rekawa<sup>1</sup>  
<sup>1</sup>Lawrence Berkeley National Laboratory, Berkeley, California, USA  
<sup>2</sup>ADC, Inc., 126 Ridge Rd, Lansing NY 14882, USA  
<sup>3</sup>Mirrorcle Technologies, Inc., 2700 Rydin Road, Unit F, Richmond, CA 94804

### Abstract

We are creating a synchrotron-based extreme ultraviolet (EUV, 13.5-nm wavelength) microscope to support advanced photomask research for the semiconductor industry. The new microscope will serve photolithography generations to the year 2020 and beyond, when printed feature sizes are expected to fall below 10 nm. Called SHARP (the SEMATECH High-NA Actinic Reticle review Project), the microscope is designed to emulate the optical properties of current and future EUV lithography tools, enabling the study of mask defects, pattern architectures, optical proximity correction, phase-shifting patterns, and more [1].

EUV lithography, a pattern-transfer technology based on 13.5-nm-wavelength light, is a leading contender for the commercial mass-production of several generations of computer chips within this decade. In this wavelength range, all materials are highly absorptive, so optical systems must operate in high vacuum and optical elements are formed from glancing-incidence mirrors, multilayer-coated Bragg reflector mirrors, or from nano-patterned, diffractive optical elements. Photomasks, which carry integrated circuit master patterns, are made from an atomically-smooth low-thermal-expansion glass substrate (typically 6 x 6 x ¼ inches) with a reflective, Mo/Si multilayer coating, topped with a patterned absorber layer. During printing, the image of the photomask pattern is projected onto a photoresist-covered wafer with 4x demagnification.

Arguably, the widespread adoption of EUV lithography has been delayed by limited light source power and the unavailability of defect free masks. Owing to their highly wavelength specific optical properties, the creation of production-quality masks relies upon dedicated EUV-wavelength mask-blank inspection and pattern-imaging tools. Currently, commercial tools are several years from deployment. This delay provides an opportunity for an industry/government partnership—SEMATECH together with Lawrence Berkeley National Laboratory (LBNL)—to create and operate the SHARP microscope as a research tool that will begin operations in early 2013.

SHARP will be the first short-wavelength microscope to combine lossless, customizable coherence control [2] with zoneplate-lens imaging; and, it will be the first to use a dynamic, MEMS based EUV mirror element. The central concept of diffraction-limited EUV imaging with zoneplate lenses has been demonstrated [3]. Ultimately, we seek to measure the detailed properties of mask patterns and features that are as small as 24 nm using objective lenses that emulate mask-side numerical aperture (NA) values up to 0.156. (This is equivalent to 6-nm wafer features and 0.625-NA imaging.)



Figure 1: SHARP instrument

### SYSTEM DESCRIPTION

The system specifications can be divided into the optics (illuminator, and imaging), and the mechanical systems required to support them. Achieving high signal-to-noise ratios depends on delivering the maximum possible light-flux into the small imaging region. To that end, SHARP's simplified design contains only essential optical elements. Mechanically, the central challenge is to achieve sub-5-nm stability between the mask and the objective lens during 1–5-second exposures, a level that is required for accurate pattern measurements.

## THE SOURCE AND ILLUMINATOR

The SHARP microscope is powered by a synchrotron bending-magnet beamline at LBNL's Advanced Light Source, with a monochromator that provides tunable wavelength and bandwidth. At its focus, the beamline delivers 14  $\mu\text{W}$  of EUV power in a bandwidth,  $E/\Delta E = 1000$ , focused to a spot size of approximately 250  $\mu\text{m}$  with horizontal and vertical angular divergences of 1.85 and 4.36 mrad, respectively, see Figure 2. A four-jaw slit is placed 2.5 m upstream of focus to decrease the beam divergence for finer coherence control when necessary. A second four-jaw slit, just upstream of the focus, blocks stray light and allows us to cut the lateral size of the beamline's focus, and thus the size of the illumination spot on the mask.

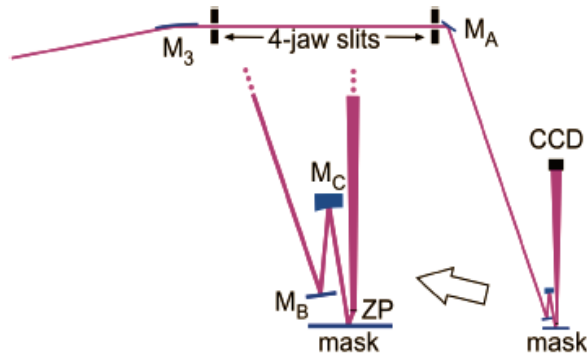


Figure 2: The beam path through the SHARP microscope. Inset detail shows a schematic of the MB, MC, the mask and the zoneplate (ZP) lens positions. The intermediate focus is on MA

### Illumination Coherence Control

To improve pattern modulation at small feature sizes, modern photolithography relies on illumination coherence control, achieved by tailoring the angular pattern of the incident light. Effective mask microscopes must emulate illumination conditions similar to printing tools. In the SHARP microscope, coherence control is achieved with a *Fourier-domain illuminator* [2] that is designed to take the narrow, static solid-angle of the synchrotron light and dynamically fill arbitrary angular patterns during the exposures, while preserving flux. The illuminator has three mirrors we refer to as MA, MB and MC, that together produce a 10x demagnification of the beamline's intermediate focus and expand the angular range of light incident on the mask up to nearly 19° off-axis (encompassing central-ray angles of 6° to 10°, or more.)

The 10x demagnification reduces the beamline's 250- $\mu\text{m}$  intermediate focus to a size that matches the microscope's typical field of view. Furthermore, the demagnification provides a 10x amplification of the range of ray angles leaving MC, simplifying the design of the illuminator.

### Dynamic EUV MEMS Mirror, MA

The flat MA mirror is a gimbal-less dual-axis, scanning MEMS device made from single-crystal silicon and

integrated onto a dual inline "DIP24" package. See Figure 3. Working with *Mirrorcle Technologies* of Richmond, California [4], we have developed a novel EUV-reflective version that can scan arbitrary angular pupil-fill patterns at speeds up to 3 kHz. The beamline's intermediate focus on MA forms a virtual source for the illuminator that is imaged onto the mask surface by the elliptical MC mirror.

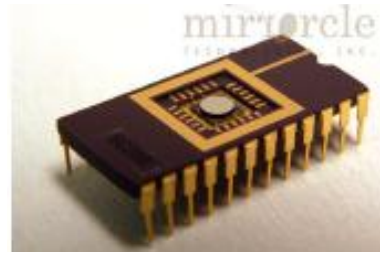


Figure 3: Mirrorcle Technologies MEMS mirror, MA

### MB and MC Mirrors

The ellipsoidal mirror MC is the heart of the illuminator, see Figure 4. It is designed for point-to-point imaging—every ray of light leaving the intermediate focus on MA reaches a single point on the mask plane. The MC mirror is being fabricated to EUV surface-finish tolerances: 0.15-nm RMS, with slope errors below 25  $\mu\text{rad}$ .

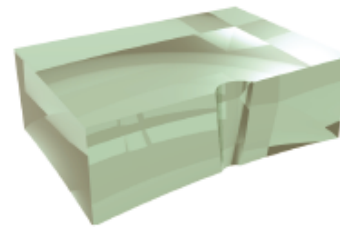


Figure 4: Model of the elliptical MC

Mirror MC is wide in the transverse direction, enabling azimuthal rotation of the angle of incidence by  $\pm 25^\circ$ . A conical hole in the one edge makes room for the upward beam path from the zoneplate to the CCD camera, see Figure 5 (a&b). The flat MB is a folding mirror that directs the beam upward into MC so the central angle of incidence on MC is 10°. MB keeps the incidence angles on MC close to normal, simplifying MC's multilayer coating.

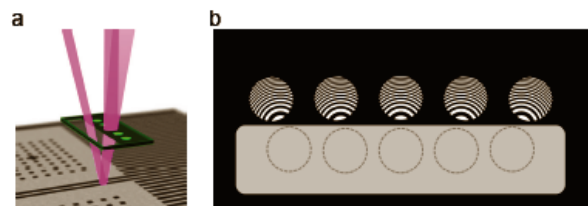


Figure 5: (a) Schematic of the beam path incident on and reflected by the mask, and then imaged by a zoneplate within a linear array (b) A schematic of an array of off-axis zoneplates designed for 5 different azimuthal orientations

The MC mirror also acts as an illumination uniformity scanner. Mounting MC on a two-axis, tiptilt stage with a peak frequency of 200 Hz enables us to steer the illumination focal point in a programmed manner across the small field of view. The total angular range of the tiptilt stage is limited to 50  $\mu$ rad, small enough not to interfere with the angular illumination patterns created for coherence control.

### *Fresnel Zoneplate Objective Lenses*

Fresnel zoneplate lenses, (typically 100- $\mu$ m diameter) project the image of the illuminated mask surface onto a 1" EUV CCD detector with high magnification. More than 70 different lenses, which are binary holograms of high (diffraction-limited) wavefront quality, are patterned in an array in a gold absorber layer on a thin silicon-nitride membrane. The array is fabricated using electron-beam lithography [5]. The zoneplates are single, off-axis lenses of various focal lengths and numerical apertures ranging from 0.0625 to 0.156. Lenses are designed for several central-ray angles and with different azimuthal rotations to mimic illumination conditions across a ring-shaped field of view in an EUV printing tool.

For zoneplates, aberration-free imaging occurs only at the center of the field of view. The width of the *sweet spot* typically covers several microns, large enough for localized defect and pattern studies of interest.

Power is critical to high-quality imaging. For a constant magnification ratio and NA, reducing the focal length shrinks the zoneplate diameter, reduces the number of zones, and thus allows a larger illumination bandwidth to be used. Since power from the beamline is proportional to the bandwidth, for constant exposure level the exposure time is proportional to the focal length. We set the nominal focal length to 500  $\mu$ m knowing we could adjust both the focal length and the distance to the CCD to achieve 4x higher magnification, if necessary.

### *Pupil-fill Monitor*

Accurate control of the mask illumination requires feedback. Space constraints in the vicinity of the illuminator's focus complicate the development of solutions above the mask plane. The limited photon flux available for conversion to visible-light motivates the positioning of scintillators within a few mm of focus, where the beam is concentrated, yet not so close that the angular pattern is unresolved. Our solution is to bond a thin (5 or 10  $\mu$ m) YAG scintillator directly to the surface of an upward facing, visible-light CCD camera that is held on the mask stage. In this configuration, the monitor could be used to assess both MC focusing (measured in the mask plane) and the pupil-fill angular distribution (below mask plane).

### *Visible-light Mask Microscope*

An *in-situ* visible-light microscope with sub-3- $\mu$ m resolution and a 1.4 x 1.0 mm field of view simplifies mask navigation, using pattern features and fiducial marks to improve position accuracy. The microscope is based on a long-working distance, 0.14-NA objective with an infinite conjugate, and a relay optical system that projects the image to a CCD camera, positioned above the chamber lid. The optical components are installed in a tube that projects downward into the vacuum chamber from above, with a window at the bottom.

## **MECHANICAL SYSTEM DESIGN**

For high-magnification, nano-scale imaging, mechanical stability during multi-second exposures is the most important factor for success. Specifically, SHARP requires a sub-5-nm relative position of the mask and zoneplate during exposure. Thus the overall mechanical design is focused on the in-vacuum vibration isolation of the mask and zoneplate stages, achieved within a noisy experimental hall, in close proximity to pumps and other equipment.

### *Vibration Isolation*

The design begins with a grouted, level floor plate that provides a common base for the chamber and the vibration-isolated platform, see Figure 6. This plate bridges a buried grade beam that is a strong source of localized floor vibrations. Studies showed floor vibration levels of 10 nm integrated RMS displacement above 2 Hz. Three TMC STACIS® 2100 active piezoelectric vibration cancellation systems support a rigid, 4-inch-thick, triangular aluminum plate in the space below the vacuum chamber. The system has an effective active resonant frequency of 0.5 Hz—the transmissibility at resonance is below 1.1 and it is designed to provide 90% isolation at 2 Hz. Inside the vacuum chamber, the unified mask and zoneplate stage support structure is attached to this aluminum plate through the bottom of the chamber using four pillars and flexible bellows. The chamber is independently supported by six struts tied to the floor plate.

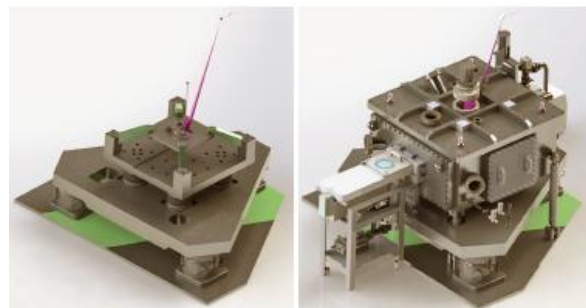


Figure 6: (Left) CAD model of SHARP's vibration-isolation system. (Right) Model of the assembled system; the beam path is shown in magenta. The green stripe represents the location of a buried grade beam.

## *Mask and Zoneplate Stage Support Frame*

The mask and zoneplate array move independently, on separate  $xyz$  stages. The  $xy$  mask stage travel exceeds 200 mm, enabling us to reach every point on the mask surface. The  $xyz$  zoneplate stage hangs down from a plate located above the mask.

## *Mask Loading, Holding and Transfer*

Mask loading occurs through a conventional robotic load-lock from *Transfer Engineering, Inc.* The mask is held onto the mask stage using a spring-loaded tab system. This system provides lateral position and angle repeatability of approximately 10  $\mu\text{m}$  and 50  $\mu\text{rad}$ . The gravitational sag of the mask supported in this manner induces an apparent tilt at the edges of the mask that is predicted to be below 16  $\mu\text{rad}$ —within the 500  $\mu\text{rad}$  mask-tilt specifications required for zoneplate alignment.

## *Zoneplate Holder*

The small zoneplate wafer ‘chips’, containing the lens arrays, will be held magnetically, flush to a level glass mounting piece using embedded magnets and a thin, electroplated Ni coating on the back side of the zoneplate array ‘chips.’ This technique will enable us to use very short zoneplate focal lengths (100–250  $\mu\text{m}$ ) without the risk of bumping the mask surface on a downward protruding clip of some kind. A zoneplate loading and unloading system will be installed on the mask  $z$  stage to exchange zoneplates without breaking vacuum.

## *Particle and Light Baffles*

It is the nature of photomasks, the carriers of nano-scale patterns, to be extremely vulnerable to particle contamination. Care has been used in the selection of stages and components to avoid particle generation wherever possible, and to shield the critical components from direct exposure to particles where possible. During its time within the chamber, the mask is protected from particles, held below a thin metal sheet, with openings only in the two critical locations where observation and inspection takes place: for the EUV zoneplate and the visible-light microscope.

Owing to the extreme sensitivity of the EUV CCD camera to visible and infrared light, internal light emissions from stage encoders and vacuum ion gauges, for example, must be curtailed, and blocked. Magnetic encoders, low heat stages, and cold cathode vacuum gauges were selected to reduce light leaks and provide the darkest possible internal environment.

## **ACKNOWLEDGEMENTS**

Plans for SHARP have grown from experience operating and upgrading its predecessor, the SEMATECH Berkeley Actinic Inspection Tool (AIT). These projects owe a debt of gratitude to semiconductor industry and engineering

research leaders, and to previous team members including John Taylor (LLNL), Anton Barty (DESY), Yanwei Liu (KLA Tencor), C. Drew Kemp, Obert Wood (GlobalFoundries), and David Chan (SEMATECH). This work was funded by SEMATECH under Agreement No. LB08005006, and is performed under the auspices of the U.S. Department of Energy by the University of California Lawrence Berkeley National Laboratory under management and operating contract DE-AC02-05CH11231.

## **REFERENCES**

- [1] Goldberg, K A, et al., An EUV Fresnel zoneplate mask-imaging microscope for lithography generations reaching 8 nm, Proc. SPIE 7969, 79691O (2011).
- [2] Naulleau, P, et al. Fourier-synthesis custom-coherence illuminator for extreme ultraviolet microfield lithography, Appl. Opt., 42 (5), 820 (2003).
- [3] Mochi, I, et al., Improving the performance of the Actinic Inspection Tool with an optimized alignment procedure, Proc. SPIE 7271, 727123 (2009).
- [4] Mirrorcle Technologies, Inc.
- [5] Chao, W, Real space soft x-ray imaging at 10 nm spatial resolution, Opt. Exp. 20 (9) 9777 (2012).